Model based control of permanent magnet AC servo motor drives

Thounthong, P.; Sikkabut, S.; Mungporn, P.; Yodwong, B.; Kumam, P.; Bizon, N.; Tricoli, P.; Nahid-Mobarakeh, B.; Pierfederici, S.

Model Based Control of Permanent Magnet AC Servo Motor Drives

P. Thounthong[1,2*], S. Sikkabut[1,3], P. Mungporn[1,3], B. Yodwong[1,3], P. Kumam[4], N. Bizon[5], P. Tricoli[6], B. Nahid-Mobarakeh[7], and S. Pierfederici[7]

[1]Renewable Energy Research Centre, King Mongkut's University of Technology North Bangkok (KMUTNB), Thailand
[2]Department of Teacher Training in Electrical Engineering, Faculty of Technical Education, KMUTNB, Bangkok, Thailand
[3]Thai-French Innovation Institute, King Mongkut's University of Technology North Bangkok, Bangkok, Thailand
[4]Department of Mathematics, King Mongkut's University of Technology Thonburi, Bangkok, Thailand
[5]Faculty of Electronics, Communications and Computers Science, University of Pitesti, Pitesti, Romania
[6]School of Electronic, Electrical and Computer Engineering, University of Birmingham, Birmingham, United Kingdom
[7]Groupe de Recherche en Electrotechnique et Electronique de Nancy, Université de Lorraine, Lorraine, France
*E-mail: phtt@kmutnb.ac.th

***Abstract*--This paper presents an innovative control law for permanent magnet synchronous motor (PMSM) drive for high dynamics applications. This kind of system (three-phase inverter connected with a PMSM) exhibits nonlinear behavior. Classically, to control the speed and the current (torque), a linearized technique is often used to study the stability and to select the controller parameters at specific operating point. In this paper, a model based control based on the flatness property of the drive system is proposed. Flatness provides a convenient framework for meeting a number of performance specifications on the PMSM drive. To validate the proposed method, a prototype PMSM drive (1 kW, 3000 rpm) is realized in the laboratory. The proposed control law is implemented by digital estimation in a dSPACE 1104 controller card. Experimental results demonstrate that the nonlinear differential flatness-based control provides improved speed/current regulation relative to a classical linear PI vector control method.**

***Index Terms*-- Flatness control, permanent magnet synchronous motor (PMSM), pulse width modulation, vector control.**

I. INTRODUCTION

PMSMs are extensively applied in rapidly developing industries owing to their fast response and highly efficient characteristics. Because power is only supplied to the stator without copper loss, it has an exceptional cooling characteristic compared with other motors. It has achieved rapid progress as a high performance and highly efficient motor [1], [2].

Control, robustness, stability, efficiency, and optimization of PMSM drives remain an essential area of research. Differential flatness theory (nonlinear approach) was first introduced by Fliess *et al.* [3]. This allowed an alternate representation of the system, where trajectory planning and nonlinear controller design is clear-cut. These ideas have been used lately in a variety of nonlinear systems across various engineering disciplines [4], [5], [6].

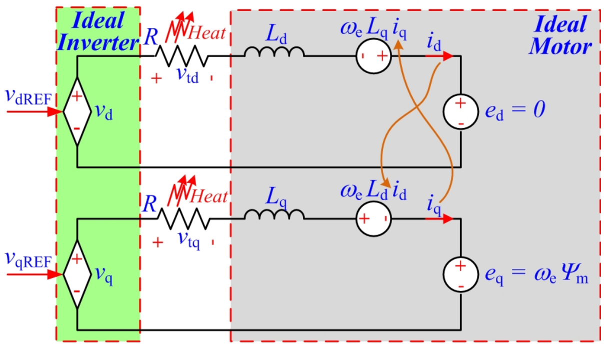

Fig. 1. An equivalent circuit of PMSM drive.

This paper presents the original control method based on the flatness properties for the speed/torque control of a PMSM drive. It will provide a significant contribution to the field of the motion control applications. In Section II, the inverter/motor model and the proposed control laws based on the differential flatness properties will be explained in detail. In Section III, experimental results will show the system performance during load cycles. The conclusions are presented in Section IV.

II. MODELING AND CONTROL

A. Mathematic Model of the PMSM/inverter

The sinusoidal pulse-width modulation technique (SPWM) is applied to an inverter in order to achieve a sinusoidal output voltage with a minimum of undesired harmonics. The power-invariant transformations from the stationary (*abc*) to the rotating reference frame (*dq*) are applied. Ignoring magnetic saturation, in *dq*-synchronous rotating frames, the equipvalent circuit of PMSM inverter drive is shown in Fig. 1 and the differential equations of PMSM/inverter can be written as [7], [8]:

$$\frac{di_d}{dt} = \frac{1}{L_d}\left(v_d - R \cdot i_d + \omega_e \cdot L_q \cdot i_q\right) \tag{1}$$

$$\frac{di_q}{dt} = \frac{1}{L_q}\left(v_q - R \cdot i_q - \omega_e \cdot L_d \cdot i_d - \omega_e \cdot \Psi_m\right) \tag{2}$$

This work was supported in part by a research program in cooperation with the Thai-French Innovation Institute, King Mongkut's University of Technology North Bangkok (Thailand), with the Université de Lorraine (France) under Contract KMUTNB-60-GEN-035.

$$\frac{d\omega_{\mathrm{m}}}{dt} = \frac{1}{J}\left(T_{\mathrm{e}} - B\cdot\omega_{\mathrm{m}} - T_{\mathrm{L}}\right) \quad (3)$$

with,

$$T_{\mathrm{e}} = p\cdot i_{\mathrm{q}}\cdot\left(\Psi_m - \left(L_{\mathrm{q}} - L_{\mathrm{d}}\right)\cdot i_{\mathrm{d}}\right) \quad (4)$$

$$\omega_{\mathrm{e}} = p\cdot\omega_{\mathrm{m}} \quad (5)$$

where, i_{d} and i_{q} the direct and quadrature motor currents (A); Ψ_{m} the permanent magnet flux linkage (Wb); L_{d} the d-axis inductance (H); L_{q} the q-axis inductance (H); ω_{e} is the electrical angular frequency (rad/s); ω_{m} the mechanical angular frequency (rad/s); p the number of pole pairs; T_{e} the electromagnetic torque (Nm); T_{L} the load torque (Nm); B is the friction coefficient (Nm·s/rad); and J is the moment of inertia of the rotor. It should be noted here that a PMSM is always driven by a three-phase inverter; for this reason, R is simplified as losses in an inverter (static and dynamics losses; switching deadtime; voltage drops in IGBTs and Diodes) and in a PMSM (the stator winding resistance, hysteresis losses, and eddy current losses).

B. Current Control Loop

As mentioned in *section II. A*, $L = L_{\mathrm{d}} = L_{\mathrm{q}}$ and refer to equations (3) and (4). To prove that the system is flat [6], [9], one defines the flat output $\boldsymbol{y} = [y_1, y_2]^{\mathrm{T}}$, control variable $\boldsymbol{u} = [u_1, u_2]^{\mathrm{T}}$, and state variable $\boldsymbol{x} = [x_1, x_2]^{\mathrm{T}}$ as follows:

$$\mathbf{y} = \begin{bmatrix} i_{\mathrm{d}} \\ i_{\mathrm{q}} \end{bmatrix},\ \mathbf{u} = \begin{bmatrix} v_{\mathrm{d}} \\ v_{\mathrm{q}} \end{bmatrix},\ \mathbf{x} = \begin{bmatrix} i_{\mathrm{d}} \\ i_{\mathrm{q}} \end{bmatrix} \quad (6)$$

Then, the state variables of **x** can be written as

$$\mathbf{x} = \begin{bmatrix} \varphi_1(y_1) \\ \varphi_2(y_2) \end{bmatrix} \quad (7)$$

From (1) and (2), the control variables of **u** can be calculated from the flat outputs **y** and its time derivatives (inverse dynamics [6]):

$$\begin{aligned} u_1 &= L\cdot\dot{i}_{\mathrm{d}} + R\cdot i_{\mathrm{d}} - \omega_{\mathrm{e}}\cdot L\cdot i_{\mathrm{q}} = \psi_1(y_1, \dot{y}_1, y_2) \\ &= v_{\mathrm{dREF}} \end{aligned} \quad (8)$$

$$\begin{aligned} u_2 &= L\cdot\dot{i}_{\mathrm{q}} + R\cdot i_{\mathrm{q}} + \omega_{\mathrm{e}}\cdot L\cdot i_{\mathrm{d}} + \omega_{\mathrm{e}}\cdot\Psi_{\mathrm{m}} \\ &= \psi_1(y_1, y_2, \dot{y}_2) = v_{\mathrm{qREF}} \end{aligned} \quad (9)$$

Desired references for the *dq*-currents are represented by y_{1REF} (= i_{dREF}) and y_{2REF} (= i_{qREF}). Feedback control laws achieving an exponential asymptotic tracking of the set-points are given by the following expression [5]:

$$\left(\dot{y}_1 - \dot{y}_{\mathrm{1REF}}\right) + K_{11}\left(y_1 - y_{\mathrm{1REF}}\right) + K_{12}\int_0^t \left(y_1 - y_{\mathrm{1REF}}\right)d\tau = 0 \quad (10)$$

$$\left(\dot{y}_2 - \dot{y}_{\mathrm{2REF}}\right) + K_{11}\left(y_2 - y_{\mathrm{2REF}}\right) + K_{12}\int_0^t \left(y_2 - y_{\mathrm{2REF}}\right)d\tau = 0 \quad (11)$$

where K_{11} and K_{12} are the controller parameters. One may set the following as a desired characteristic polynomial:

$$p(s) = \mathrm{s}^2 + 2\zeta_1\omega_{\mathrm{n1}}\mathrm{s} + \omega_{\mathrm{n1}}^2\,; \quad (12)$$

$$K_{11} = 2\zeta_1\omega_{\mathrm{n1}} \quad ;\ K_{12} = \omega_{\mathrm{n1}}^2 \quad (13)$$

where ζ_1 and ω_{n1} are the desired dominant damping ratio and natural frequency and new variables are defined $\lambda_1 = \dot{y}_1$ and $\lambda_2 = \dot{y}_2$.

Trajectory planning is an important step in the implementation of a flatness-based control. It is thus noteworthy to give a well-known waveform such that all the transient state behaviors can be predicted. Next, to limit the transient current, a second order filter is used such that the current command i_{COM} is always limited by

$$\frac{i_{\mathrm{REF}}(s)}{i_{\mathrm{COM}}(s)} = \frac{1}{\left(\dfrac{s}{\omega_{\mathrm{n2}}}\right)^2 + \dfrac{2\zeta_2}{\omega_{\mathrm{n2}}}s + 1} \quad (14)$$

where ζ_2 and ω_{n2} are the desired dominant damping ratio and natural frequency.

C. Speed Control Loop

The outer loop concerns the speed regulation where the flat output is chosen as $y_3 = \omega_{\mathrm{m}}$, a control variable $u_3 = i_{\mathrm{q}}$, and a state variable $x_3 = \omega_{\mathrm{m}} = \varphi_3(y_3)$. So, the flatness based speed controller output generates the command of the q-axis current, i_{qCOM}. According to mechanical equations (3) – (5), and on the assumption that i_{q} (= y_2) = i_{qCOM} because the inner current loop bandwidth is estimated to be faster than the bandwidth of the external speed loop, control variable u_3 (=i_{qCOM}) can be expressed in an *inverse dynamics term* as:

$$\begin{aligned} u_3 &= \left(J\cdot\dot{\omega}_{\mathrm{m}} + T_{\mathrm{L}} - B\cdot\omega_{\mathrm{m}}\right)/\,p\cdot\Psi_{\mathrm{m}} = \psi_3(y_3, \dot{y}_3) \\ &= i_{\mathrm{qCOM}} \end{aligned} \quad (15)$$

It is similar to the inner current control loops. A desired reference for the mechanical speed is represented by y_{3REF} (= ω_{mREF}). A feedback control law is given by the following expression:

$$\lambda_3 = \dot{y}_{\mathrm{3REF}} + K_{21}\left(y_{\mathrm{3REF}} - y_3\right) + K_{22}\int_0^t \left(y_{\mathrm{3REF}} - y_3\right)d\tau \quad (16)$$

where $K_{21} = 2\zeta_3\omega_{\mathrm{n3}}$ and $K_{22} = \omega_{\mathrm{n3}}^2$. (17)

Finally, in view of the nature of the derived feedback control law (16) , we need to generate the current command for the inverter. Because our focus is on a smooth accelerator or brake (known as a soft-start system), we restrict the reference profiles to smooth changes between stationary regimes. Next, the motion trajectory planning is defined as

$$\frac{\omega_{\mathrm{REF}}(s)}{\omega_{\mathrm{COM}}(s)} = \frac{1}{\left(\dfrac{s}{\omega_{\mathrm{n4}}}\right)^2 + \dfrac{2\zeta_4}{\omega_{\mathrm{n4}}}s + 1} \quad (18)$$

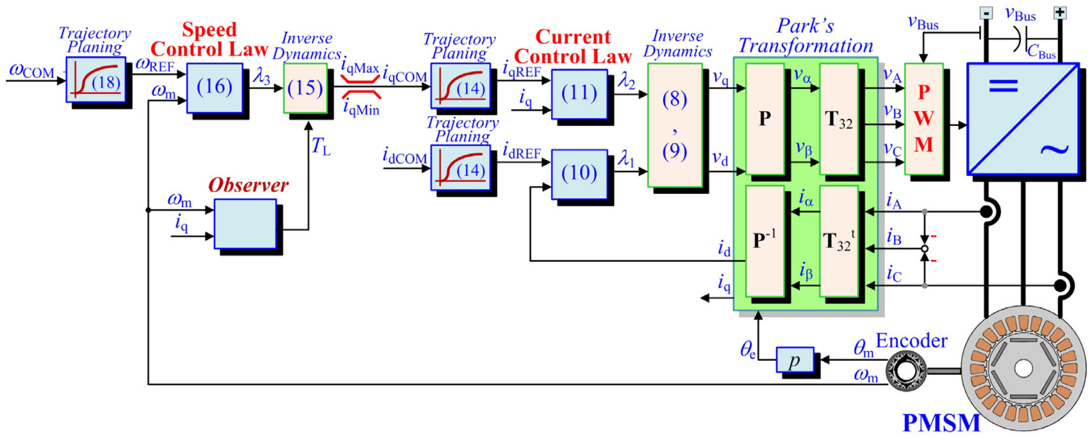

Fig. 2. Proposed a differential flatness based speed/torque control of a PMSM drive.

D. Control Conclusion

In Fig. 2, the proposed control algorithm, as detailed earlier, is depicted. The external speed control algorithm generates a current command i_{qCOM}. This signal must be saturated within an interval [i_{qMax}, i_{qMin}]. The inner current control algorithm estimates the voltage references. These result in voltage references v_d and v_q.

Based on the power electronic constant switching frequency ω_S and cascade control structure, the outer speed control loop must operate at a cutoff frequency $\omega_{n3} << \omega_{n2} << \omega_{n1} << \omega_S$ [6]. However, to increase the speed respose, one may set $\omega_{n4} = \omega_{n3}$. For system damping ratios, one may set $\zeta_4 = \zeta_3 = \zeta_2 = \zeta_1 = 1$ pu. Once the flat outputs are stabilized, the whole system is stable because all the variables of the system are expressed in terms of the flat outputs.

Moreover, for the *inverse dynamics term* (15), the proposed control algorithm needs to estimate the load torque T_L. Then, a classic linear observer named "the disturbance observer" is implemented [10].

III. Experimental Validation

In order to authenticate the proposed control algorithm and control laws, a small-scale test bench of the PMSM drive was implemented in our laboratory, as presented in Fig. 3. The PMSM used in this effort was a brushless AC servomotor (1 kW, 3000 rpm; LEROY SOMER MOTOR). The three-phase inverter was initially designed for more general purposes, so that three IGBT module SKM50GB123D (SEMIKRON: 1200 V, 50 A) are used for six switches S_1–S_6. The PMSM/Inverter specification and parameters are presented in Table I used for following experimentations. The machine parameters were obtained from the *offline identifications*, in which the PMSM was connected with the inverter. For this reason, the simplified resistance R is quite high, because it represents some losses in the cables, the inverter, and motor.

Parameters associated with the speed/torque regulation loops can be seen in Table II. Moreover, these control loops, which generated voltage references v_d and v_q, were implemented in the real-time card dSPACE DS1104 (see Fig. 3) using MATLAB–Simulink.

A. Inner Current Control Loop Test

First, the performance comparison between a classical linear control and a nonlinear control based on a differential flatness approach for current i_d and i_q regulation of a PMSM drive is presented as follows. A classic PI tranfer function for the current control is given by

$$\mathrm{PI}_i(s) = K_{Pi} + \frac{K_{Ii}}{s} \tag{19}$$

where K_{Pi} and K_{Ii} are the controller parameters. To give a practical comparison between the control methods, the parameters of the linear controller K_{Pi} and K_{Ii} were tuned to obtain the best possible performance [1]. In this case, K_{Pi} = 8 V·A^{-1}, and K_{Ii} = 3316 V·(As)$^{-1}$. For the differential flatness approach, the nonlinear controller gains used were K_{11} = 3000 rad · s^{-1} and K_{12} = 2500000 rad^2 · s^{-2} (ζ_1 = 1 and ω_{n1} = 1500 rad · s^{-1}), see table II.

Figs. 4 and 5 show the experimental results obtained for both controllers during the current command i_{qCOM} step from -1 A to 1 A, whereas i_{dCOM} = 0 A. It should note here that for the linear PI control $i_{COM} = i_{REF}$. They shows i_{qCOM}, i_q, i_d, the speed n, the stator curents i_A and i_C. One may observe that the settling time (around 40 ms) of the current i_q from both controllers are closed; however, the current i_q response by the flatness control is smoother than the PI control.

B. Speed/Current Control Loop Test

To compare the performance of the flatness-based speed control, a traditional linear control method was also implemented on the test stand. A linear feedback PI tranfer function is given by the following expression:

$$\mathrm{PI}_n(s) = K_{Pn} + \frac{K_{In}}{s} \tag{20}$$

where K_{Pn} and K_{In} are the controller parameters. To give a practical comparison between the control methods, the parameters of the linear controller K_{Pn} and K_{In} were tuned to obtain the best possible performance [1]. In this case,

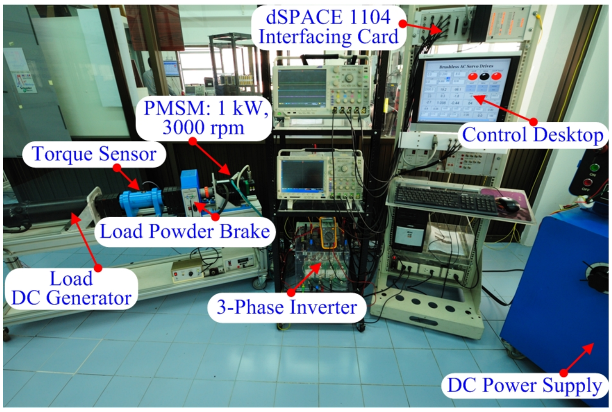

Fig. 3. Test bench of the PMSM drive.

Table I. PMSM/Inverter specification and parameters.

Rated Power P_{rated}	1000	W
Rated Speed n_{rated}	3000	rpm
Rated Torque T_{rated}	3	Nm
Number of poles pair p	3	
Resistance (Motor+Inverter) R	8.77	Ω
Stator inductance $L = L_d = L_q$	19.3	mH
Magnetic flux Ψ_m	0.2214	Wb
Equivalent inertia J	4.75×10^{-3}	kg· m^2
Viscous friction coefficient B	0.99×10^{-3}	Nm· s/rad
V_{Bus}	540	V
Switching Frequency f_S	10	kHz

Table II. Speed/current regulation parameters.

ζ_1	1	pu.
ω_{n1}	1500	rad· s^{-1}
ζ_2	1	pu.
ω_{n2}	150	rad· s^{-1}
ζ_3	1	pu.
ω_{n3}	15	rad· s^{-1}
ζ_4	1	pu.
ω_{n4}	15	rad· s^{-1}
i_{qMax}	+6	A
i_{qMin}	−6	A

K_{Pn} = 0.2 As·rad^{-1}, and K_{In} = 4 A·rad^{-1}. For the differential flatness approach, the nonlinear controller gains used were $K_{21} = 30$ rad · s^{-1} and $K_{22} = 250$ rad^2 · s^{-2} ($\zeta_1 = 1$ and $\omega_{n1} = 15$ rad · s^{-1}), see table II. It should note here that, for the linear PI speed control, the speed trajectory planning is also defined in (18).

Figs. 6 and 7 show the experimental results obtained for both controllers during the speed command n_{COM} step from -1500 r/min to 1500 r/min, whereas i_{dCOM} = 0 A. They shows the speed command n_{COM}, the speed reference n_{REF}, the speed n, i_q, i_d, and the stator curent i_A. For the PI speed control, the speed settling time is around 0.7 s. For the flatness speed control, the speed settling time is around 0.6 s. One may observe that the settling time of the speed by the flatness control is faster than the PI control. Moreover, the current i_d pertubation during speed transition by the flatness control is lower than the PI control.

Finally, Figs. 8 and 9 show experimental results obtained for both controllers during the large load torque step at the speed command of 1000 r/min. The oscilloscope waveforms in Figures show: Ch1: the speed reference n_{REF}; (= n_{COM}) Ch2: the speed measurment n; Ch3: the q-axis current reference i_{qREF}; Ch4: the q-axis current i_q; Ch5: the d-axis current i_d; Ch6: the phase current i_A; Ch7: the phase current i_C; and the trajectories of the transient stator current vector. For the PI speed control, the speed settling time is around 0.3 s. For the flatness speed control, the speed settling time is around 0.16 s. The flatness-based control shows good stability and optimum response of the speed regulation to its desired reference. Although dynamic response of the linear control law could be improved relative to that shown in the figures, this enhancement comes at the expense of a reduced stability margin. From the results above, we conclude that flatness-based control provides better performance than the classical PI controller.

IV. Conclusions

The proposed control approach, based on the differential flatness control, presents the dynamics, stability, and efficiency of the PMSM drive. The average model of the PMSM drive system is flat. A trajectory planning algorithm that allows for speed/torque regulation in finite time has also been presented. Theoretically, the flatness-based control shows better performance than a classical controller (PI controllers) for transitions between equilibrium points, particularly in a nonlinear system.

Finally, the nonlinear flatness-based control is a model-based control approach. It requires to know system parameters (such stator resistance, etc.) to obtain the differential flatness property [refer to the dynamics term (8), (9)]. For future works, some online state observers (or parameter observers) including improved load torqe observer will be studied to progress the system performance.

References

[1] Sheng-Ming Yang and Kuang-Wei Lin, "Automatic Control Loop Tuning for Permanent-Magnet AC Servo Motor Drives," *IEEE Trans. Ind. Electron*., vol. 63, no. 3, pp. 1499–1506, Mar. 2016.

[2] N. Bizon, L. Dascalescu, and N. M. Tabatabaei (Ed.), Autonomous Vehicles: Intelligent Transport Systems and Smart Technologies, Nova Science Publishers Inc., USA, 2014, ISBN: 978-1-63321-324-1, pp. 541.

[3] M. Fliess, J. Levine, P. h. Martin, and P. Rouchon, "A Lie–Bäcklund approach to equivalence and flatness of nonlinear systems," *IEEE Trans. Automat. Contr*., vol. 44, no. 5, pp. 922–937, May 1999.

[4] M. A. Danzer, J. Wilhelm, H. Aschemann, and E. P. Hofer, "Model-based control of cathode pressure and oxygen excess ratio of a PEM fuel cell system," *J. Power Sources*, vol. 176, no. 2, pp. 515–522, Feb. 2008.

[5] P. Thounthong, P. Tricoli, and B. Davat, "Performance investigation of linear and nonlinear controls for a fuel cell/supercapacitor hybrid power plant," *Int. J. Elect. Power Energy Syst*., vol. 54, pp. 454–464, Jan. 2014

[6] P. Thounthong *et al*., "DC bus stabilization of li-ion battery based energy storage for a hydrogen/solar power plant for autonomous network applications," *IEEE Trans. Ind. Appl*., vol. 51, no. 4, pp. 2717–2725, Jul./Aug. 598 2015.

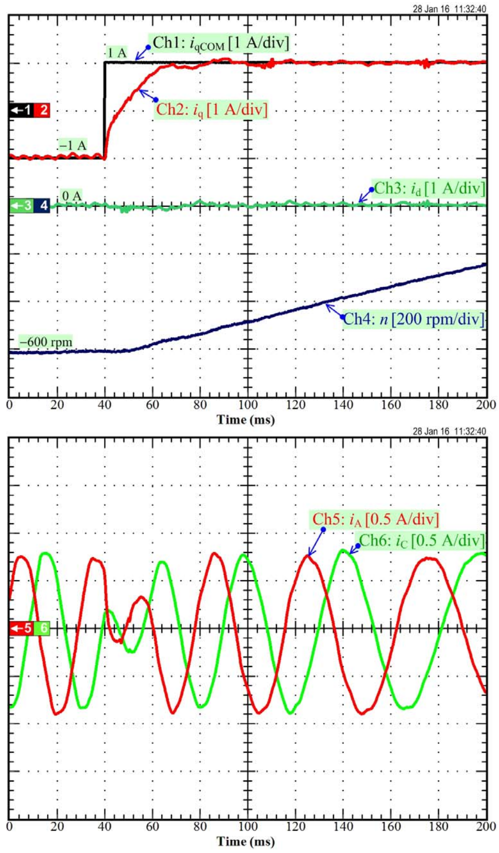

Fig. 4. Experimental result: PI based current control at a current i_{qCOM} step from −1 A to 1 A.

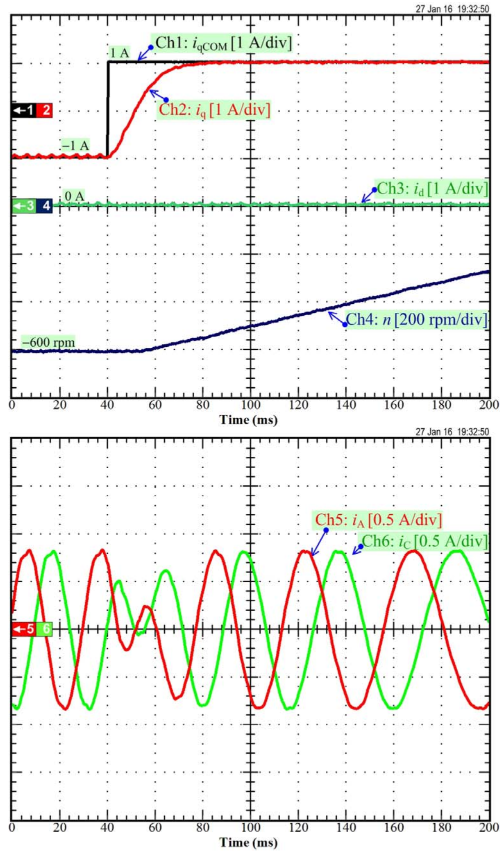

Fig. 5. Experimental result: Flatness based current control at a current i_{qCOM} step from −1 A to 1 A.

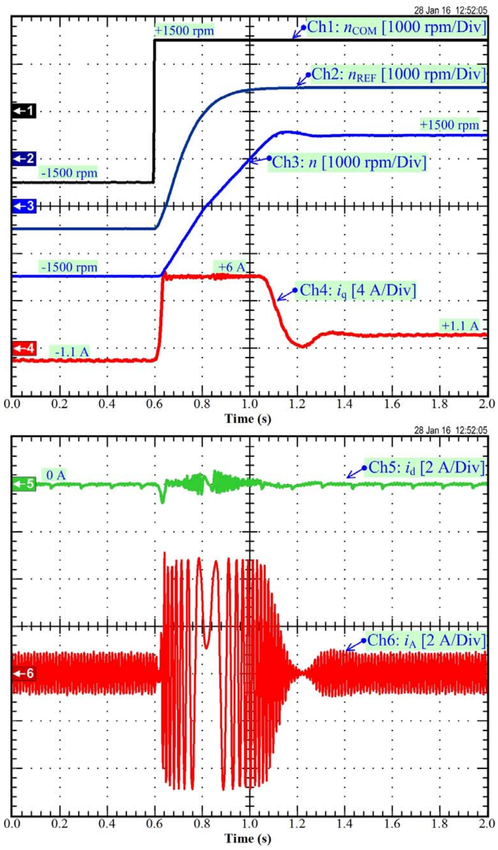

Fig. 6. Experimental result: PI based speed/current control at a speed n_{COM} step from −1500 r/min to 1500 r/min.

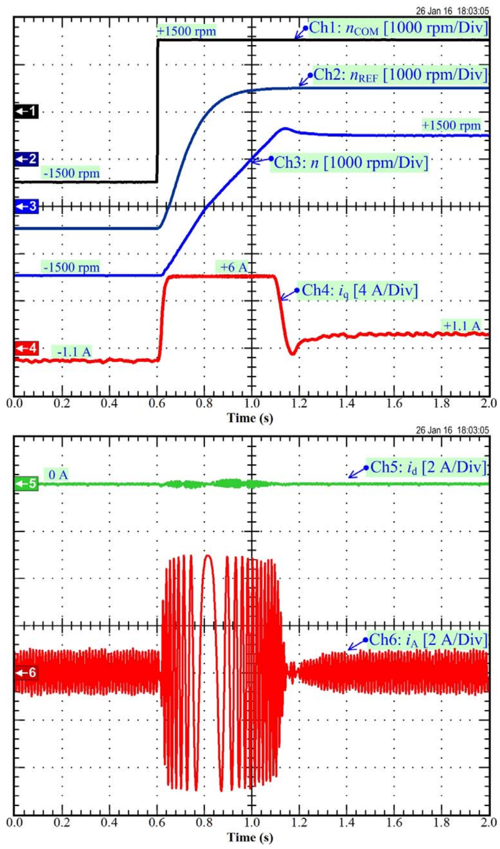

Fig. 7. Experimental result: flatness based speed/current control at a speed n_{COM} step from −1500 r/min to 1500 r/min.

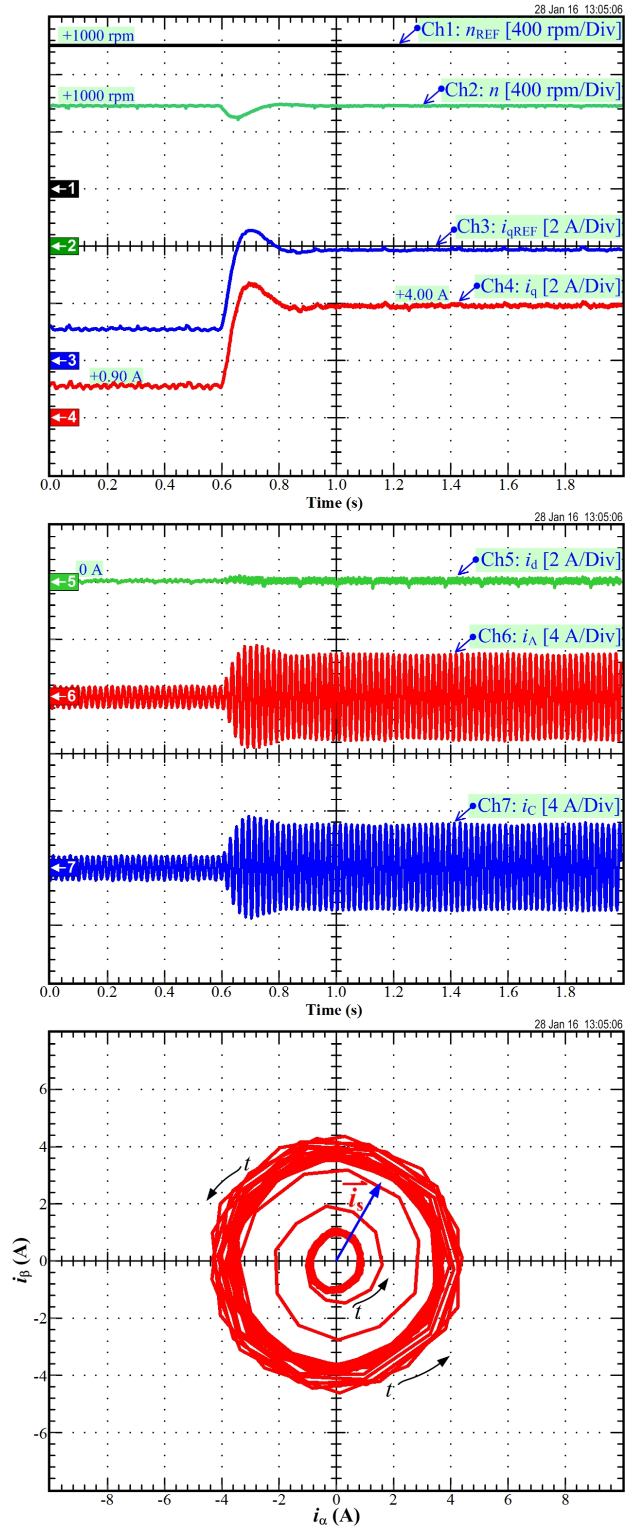

Fig. 8. Experimental result: PI based speed/current control at a speed regulation of 1000 r/min and a load torque step from 0.6 Nm to 2.66 Nm.

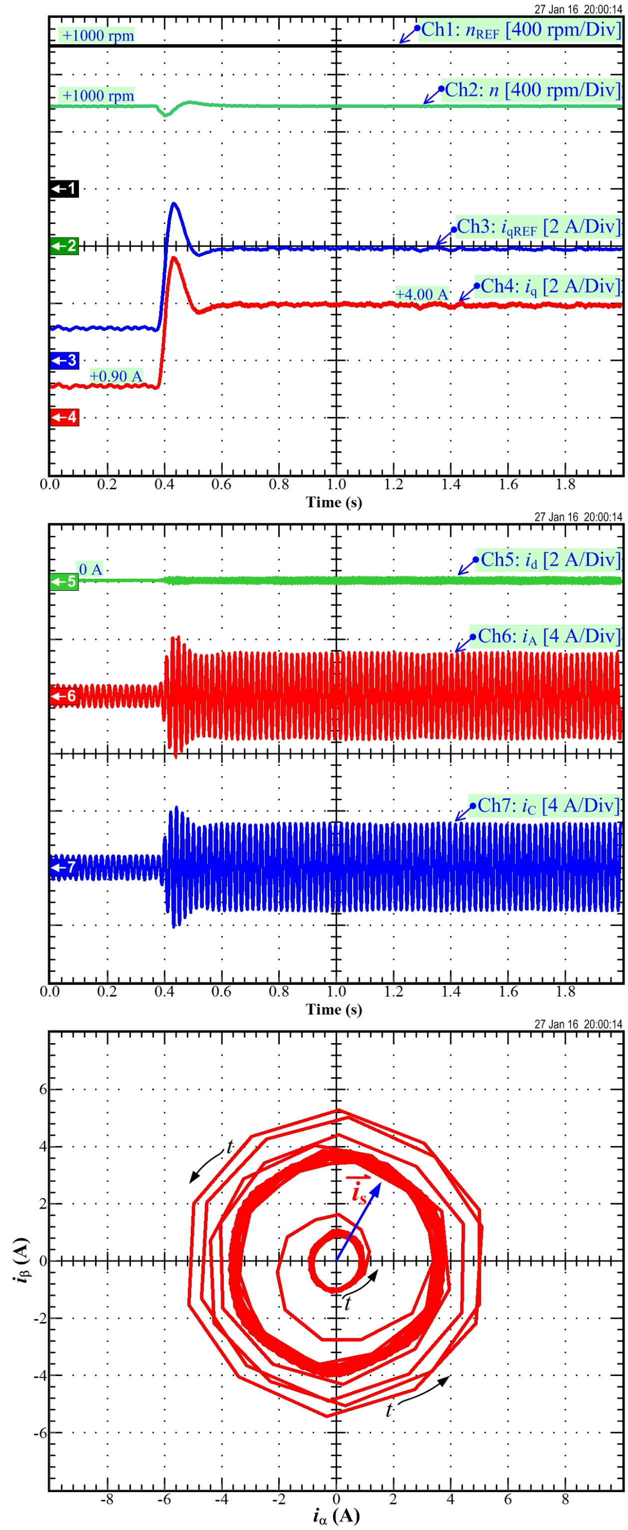

Fig. 9. Experimental result: flatness based speed/current control at a speed regulation of 1000 r/min and a load torque step from 0.6 Nm to 2.66 Nm.

[7] M. A. Shamsi-Nejad, B. Nahid-Mobarakeh, S. Pierfederici, and F. Meibody-Tabar, "Fault Tolerant Permanent Magnet Drives: Operating Under Open-circuit and Shortcircuit Switch Faults," *KMUTNB Int J Appl Sci Technol*, vol. 7, no.1, pp. 57-64, 2014. DOI: 10.14416/j.ijast.2014.01.007.

[8] A. Battiston *et al.*, "A control strategy for electric traction systems using a PM-motor fed by a bidirectional z-source inverter," *IEEE Trans. Veh. Technol.*, vol. 63, no. 9, pp. 4178–4191, Nov. 2014.

[9] E. Song, A. F. Lynch, and V. Dinavahi, "Experimental validation of nonlinear control for a voltage source converter," *IEEE Trans. Control Syst. Technol.*, vol. 17, no. 5, pp. 1135–1144, Sep. 2009.

[10] K. Ohnishi, M. Shibata, and T. Murakami, "Motion control for advanced mechatronics," *IEEE/ASME Trans. Mechatronics*, vol. 1, no. 1, pp. 56–67, Mar. 1996.